Eur Radiol (2004) 14:937–944
DOI 10.1007/s00330-004-2258-8

Thomas M. Keller
Sven C. A. Michel
Johannes Fröhlich
Daniel Fink
Rosmarie Caduff
Borut Marincek
Rahel A. Kubik-Huch

USPIO-enhanced MRI for preoperative staging of gynecological pelvic tumors: preliminary results

Received: 8 September 2003
Revised: 31 December 2003
Accepted: 9 January 2004
Published online: 26 February 2004

T. M. Keller · S. C. A. Michel
B. Marincek · R. A. Kubik-Huch
Institute of Diagnostic Radiology,
Zurich University Hospital,
Zurich, Switzerland

J. Fröhlich
Guerbet Group,
Zurich, Switzerland

D. Fink
Department of Gynecology,
Zurich University Hospital,
Zurich, Switzerland

R. Caduff
Department of Pathology,
Zurich University Hospital,
Zurich, Switzerland

R. A. Kubik-Huch (✉)
Department of Radiology,
Kantonsspital Baden,
5404 Baden, Switzerland
e-mail: rahel.kubik@ksb.ch
Tel.: +41-56-4863803
Fax: +41-56-4863809

Abstract The aim of this study was to assess nodal enhancement with ultrasmall superparamagnetic iron oxide (USPIO)-enhanced magnetic resonance imaging (MRI) during preoperative staging of gynecological pelvic tumors within the same imaging session for the primary tumor. Pelvic MRI was performed 18–28 h after intravenous infusion of USPIO (Combidex/Sinerem, 2.6 mg Fe/kg body weight) in 13 women (mean age 51 years) scheduled for surgery for biopsy proven (n=11) or clinically suspected (n=2) uterine carcinoma. Axial T1-weighted spin-echo (SE), T2-weighted fast SE (FSE; with fat saturation), fast spoiled gradient-recalled (FSPGR) echo, sagittal and oblique T2-weighted FSE sequences were acquired on a 1.5-T system. Lymph nodes were prospectively staged using standard criteria, i.e., size and shape, as well as USPIO enhancement. Results were correlated with histology findings. MRI correctly staged all primary uterine tumors. In one case, the preoperative diagnosis of stage IV switched the therapeutic approach to radiochemotherapy. Ninety-one (86 benign, 5 malignant) of the histologically characterized nodes could be correlated with their MRI counterparts. One node was false positive; three micrometastases greater than 5 mm and one 5-mm metastasis were missed. On a nodal basis, the sensitivity score was 0.33 and the specificity score, 0.99. On a patient basis, the sensitivity score was 0.25 and the specificity score, 0.80. Our preliminary results indicate that USPIO-enhanced pelvic MRI for preoperative nodal assessment is feasible within one imaging session for primary tumors and that it has a high specificity. However, the low sensitivity in the present study is a limitation for the clinical application of this technique.

Keywords Lymph node · Lymphography · MRI · Contrast agent · USPIO · Cervical · Endometrial carcinoma · Uterus · Tumor staging

Introduction

Primary tumor staging and nodal status are critical to treatment planning and prognosis in uterine tumors, e.g., in cervical carcinoma where primary radiotherapy alone is the treatment of choice for positive lymph nodes [1]. In addition to histologic grade and other factors, e.g., myometrial invasion in endometrial carcinoma or lesion volume in cervical carcinoma, lymph node metastases are a significant prognostic factor [2–5]. Staging follows the International Federation of Gynecology and Obstetrics (FIGO) classification [6] and the TNM system [7].

Magnetic resonance imaging (MRI) is a reliable method for staging gynecological pelvic tumors [8, 9]. However, like computed tomography (CT), it is less suited for assessing pelvic lymph node status. The major

malignancy marker is a short-axis diameter of less than 1 cm [10, 11]. However, false-negative results for normal-sized malignant nodes and the impossibility of differentiating between similarly hyperplastic metastatic vs non-metastatic nodes impair staging performance [12]. Gadolinium (Gd) enhancement does not help in this regard [13]. The continuing absence of a reliable imaging method leaves surgical lymphadenectomy as the effective but invasive gold standard for lymph node staging in uterine carcinoma.

The use of dextran-coated ultrasmall superparamagnetic iron oxide (USPIO) particles may enhance the performance of preoperative MRI in noninvasive staging. USPIO is a lymph node-specific contrast agent under clinical development as a contrast agent for intravenous MR lymphography [14–16] among other indications. After intravenous injection it extravasates into the interstitial space before being transported to the lymph nodes where in healthy nodes, it is taken up by macrophages, resulting in signal loss—in contrast to a persistent signal received from metastatic nodes [17]. Several clinical studies in head and neck, mediastinal, and breast cancer have confirmed that USPIO-enhanced MRI improves the detection of lymph node metastases [16, 18–22].

Other groups have assessed USPIO for pelvic lymph node detection in urologic and pelvic cancers, but they included only one or two cases of uterine tumor [12, 23]. Our purpose was to perform a dedicated prospective study in patients with gynecological pelvic tumors specifically to explore the feasibility and utility of USPIO in preoperative primary tumor staging and lymph node mapping.

Materials and methods

Thirteen women [age 51±14 years (mean ± 1 standard deviation), range 32–73; height 163±6 cm, range 151–171; weight 66±14 kg, range 48–90] with biopsy proven carcinoma of the cervix (n=7), uterine corpus (n=3), or vulva (n=1), or uterine tumor suspected on clinical and ultrasound or CT grounds (n=2), were included in a prospective phase IIIb study. All were scheduled for surgery at the time of inclusion. Noninclusion criteria were pregnancy or lactation, standard contraindications to MRI, known allergy to dextrans or drugs containing iron salts, or a strong allergic disposition. Our institutional review board approved the protocol, and we obtained written informed consent from all patients prior to study entry.

The contrast agent [ferumoxtran (USAN); AMI-227; Combidex/Sinerem, Advanced Magnetics, Inc., Boston, USA and Guerbet, Roissy, France] was administered intravenously through a filter as a slow drip infusion (2.6 mg Fe/kg body weight diluted in 100 ml 0.9% saline solution) using a flow rate of 2–4 ml/min [22]. The average total infusion time was 45 min. The pelvic region was imaged on a 1.5-T MR system (Signa CV or Horizon, GEMS, Milwaukee, Wis.) 18–28 h later using a pelvic or torso phased-array coil. The following 2D sequences were acquired after a localizer: (a) axial T1-weighted spin-echo [SE; TR 350–500 ms, TE 8 ms, matrix 256×256, field of view (FOV) 24–28 cm, slice thickness/gap 5–6/1 mm]; (b) axial (with fat saturation) and sagittal (without fat saturation) T2-weighted fast SE [FSE; TR 3,000–6,000 ms, TE 100 ms, matrix 512×512, FOV 24–28 cm, slice thickness/gap 5–6/1 mm (axial) or 4–5/1 mm (sagittal)]; and (c) axial fast spoiled gradient-recalled (FSPGR) echo sequences [TR 80 ms, TE 8 ms (first seven patients), or TR 255 ms, TE 4 ms (last six patients, to minimize problems with chemical shift artifacts), flip angle 40°, matrix 256×256, FOV 24–28 cm, slice thickness/gap 5–6/1 mm]. All axial planes were acquired from the aortic bifurcation to the ischial tuberosity using an identical table position, slice thickness and intersection gap. Subsequently, for primary tumor staging in all cases of cervical carcinoma, we performed an axial-oblique (perpendicular to the cervical canal) T2-weighted FSE sequence (TR 3,300–5,500 ms, TE 100 ms, matrix 512×512, FOV 20–24 cm, slice thickness/gap 3.5–4/0.5–1 mm). In all cases of uterine corpus tumor, additional Gd-enhanced sagittal T1-weighted SE sequences (TR 460 or 540 ms, TE 8 or 20 ms, matrix 256×256, FOV 20–24 cm, slice thickness/gap 5/1 mm; Gd-DTPA, Magnevist, Schering AG, Berlin, Germany, 0.1 mmol/kg body weight) were acquired.

All image data were transferred to a Sun microsystems console (Advantage Workstation 3.1, GEMS, Milwaukee, Wis.) for prospective nodal analysis. In each case, all lymph nodes from the aortic bifurcation to the iliac region were assessed, including the inguinal nodes in the case of vulvar carcinoma, given the usual pattern of metastatic spread in such tumors. To identify small nodes and improve differentiation between lymph nodes and the many vessels in this region, we synchronized the axial T1-weighted SE, T2-weighted FSE and FSGPR, and sagittal T2-weighted sequences, and cross-referenced the images. We characterized lymph nodes by size and USPIO enhancement. We measured size on T1-weighted SE images to minimize interference with susceptibility effects (metastasis=short axis diameter >10 mm [10, 11]). We analyzed nodal USPIO uptake primarily on the gradient-echo sequence. In our clinical study setting, the intention was to perform primary tumor and lymph node staging in one imaging session, no pre-USPIO images were available. Thus in contrast to most previous studies, USPIO uptake could not be characterized by comparing native and USPIO-enhanced images. We considered lymph nodes showing homogeneous USPIO uptake or rim enhancement on gradient-echo sequences as benign, and those showing heterogeneous or absent USPIO uptake as malignant [22]. Thus each lymph node was classified as benign or malignant by USPIO enhancement, numbered and documented on film. Morphological criteria were recorded; however, decision making was based finally on USPIO enhancement. A consensus diagnosis was reached by a board-certified radiologist and a resident experienced in MRI, both blinded to the clinical findings. Primary tumors were staged separately by a board-certified radiologist experienced in genitourinary imaging from hard-copy films using standard criteria [24–27].

The MR T and N staging results, including the detailed mapping of suspected malignant lymph nodes, were reported preoperatively to the referring physician. Surgery was performed in all but one case, a patient with an undifferentiated sarcoma of the cervix whose preoperative imaging showed advanced spread. A biopsy only was done and the patient was then referred for radiochemotherapy (Fig. 4). No lymphadenectomy was performed in two other cases: a suspected uterine sarcoma in which an ovarian tumor was found intraoperatively (Fig. 5), and a case of cervical carcinoma treated with vaginal hysterectomy only, given the early stage (pT1a) of the primary tumor. In a fourth case, a suspected uterine tumor, hemicolectomy was performed after intraoperative discovery of cecal carcinoma invading the uterus and small intestine. These four patients were excluded from our lymph node analysis. Vulvectomy including inguinal lymphadenectomy was performed in the case of vulvar carcinoma. All other patients underwent hysterectomy and pelvic lymphadenectomy, extended in some cases to adnexectomy or appendectomy.

The final tumor diagnosis and the nodal staging histology findings were then correlated with the MRI findings. To permit node-to-node correlation, the smaller number of nodes detected—whether by MRI or histology—was defined as the total number in the patient concerned. The sensitivity, specificity and accuracy of lymph node analysis were calculated per node and per patient using Excel 1997 (Microsoft, Redmond, Wash.).

Results

MRI of the primary tumor and USPIO-enhanced imaging of the lymph nodes proved feasible in all patients. The average total examination time of 45 min was well tolerated in all cases. There were no serious reactions to USPIO. Five patients (39%) displayed mild reactions: a short episode of flush and dyspnea shortly after the start of the infusion (n=2), regressing after pausing the infusion which was then completed in both cases at a reduced flow rate (1–2 ml/min); erythema and pruritus over the injection area (n=2), resolving 10–15 min after the administration of an antihistamine combined with a steroid; and self-resolving mild itchiness and erythema on one leg (n=1). Reactions were moderate in two cases (15%): urticaria and pruritus on the trunk, neck and arms shortly after completing the infusion in one patient with a history of hay fever and erythema, resolving 1 h after oral and intravenous antihistamines and steroids; dyspnea, chest pain, pruritus and erythema in another patient shortly before completing the infusion, with spontaneous resolution 1 h later (the patient refused systemic treatment).

The final histologic diagnosis (Table 1) included cervical tumors (cervical carcinoma n=6, undifferentiated sarcoma n=1) in seven patients [stage pT1a (n=2), pT1b (n=4); the undifferentiated sarcoma was staged T4 on clinical and imaging grounds]; endometrial carcinoma (n=3: stages pT1b, pT1c and pT2b); and vulvar carcinoma (n=1: stage pT2) (Figs. 1, 2, 3, 4). Preoperative MRI correctly T-staged all these tumors. It also correctly suggested an ovarian lesion in a patient with clinical and sonographic evidence favoring uterine sarcoma (Fig. 5). Histology showed a clear-cell ovarian cystadenofibroma of borderline malignancy and endometrial hyperplasia within an endometrial polyp. In another patient with uterine carcinoma indicated by the gynecologic examination and CT findings, histology showed a cecal carcinoma (pT4) invading the uterus and small intestine. We excluded four cases from further lymph node analysis: the stage pT4 undifferentiated sarcoma of the cervix; the early cervical carcinoma which did not undergo pelvic lymphadenectomy; the clear-cell borderline ovarian cystadenofibroma; and the invasive cecal carcinoma (Table 1).

The smallest lymph nodes that could be confidently differentiated from other anatomic structures measured about 2 mm. Differentiation was problematic below this limit. MRI identified 173 lymph nodes in the 13 patients, classifying 30 as malignant by USPIO enhancement criteria (Table 1). In the nine patients retained in the final statistical analysis, MRI identified a total of 107 lymph nodes, six of which were deemed malignant (range 5–15 mm) and 101 as benign (range 2–10 mm). Histology identified a total of 186 lymph nodes, six of which were metastatic; 91 of the histologically characterized nodes could be correlated with their MRI counterparts using our study criteria; 86 were correctly staged by MRI (95% accuracy), two of which were malignant (small diameter >10 mm). One node was false-positive, while three mi-

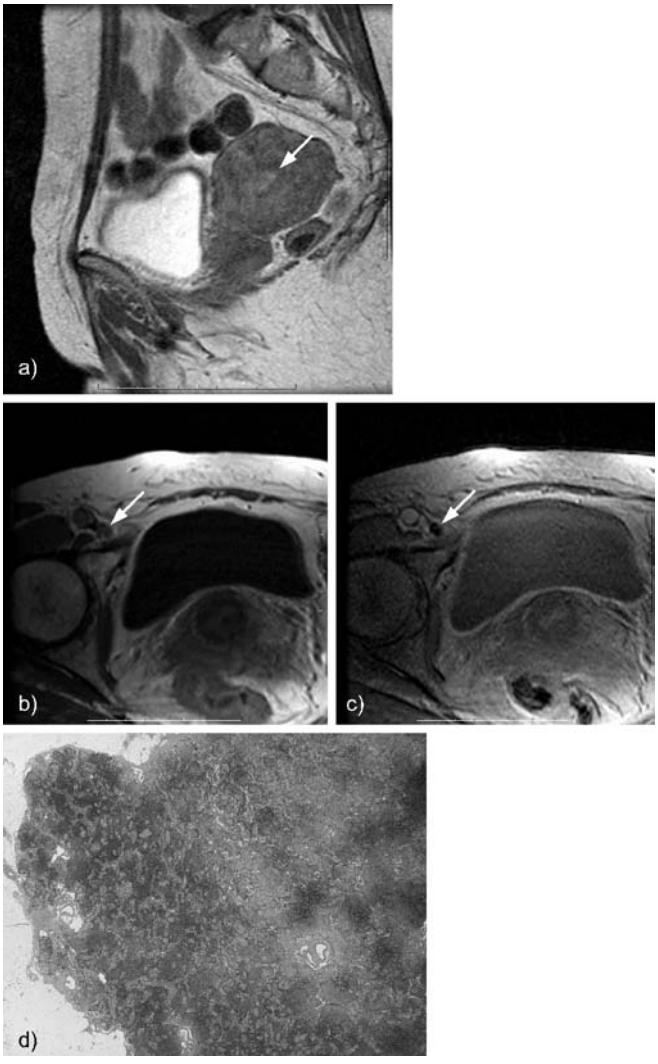

Fig. 1a–d A 65-year-old patient (no. 9, Table 1) with endometrial carcinoma (pT1b N0). **a** Sagittal Gd-enhanced T1-weighted SE (TR 540 ms, TE 20 ms), primary tumor (*arrows*); **b** axial T1-weighted SE (TR 460 ms, TE 8 ms), homogeneous USPIO uptake in all lymph nodes; **c** axial FSPGR (TR 255 ms, TE 4.2 ms, flip angle 40°), same; **d** histologic confirmation of nonmetastatic nodes. (H&E, ×10)

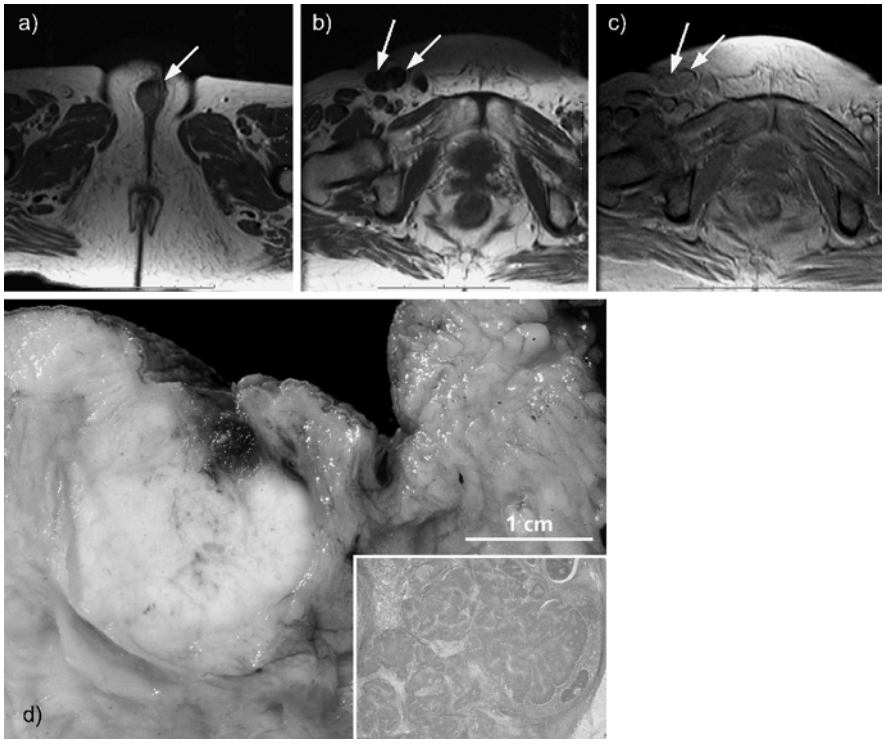

Fig. 2a–d A 72-year-old patient (no. 11, Table 1) with vulvar carcinoma (pT2 N1). **a** Axial T1-weighted SE image (TR 440 ms, TE 8 ms), primary tumor (*arrow*); **b** axial T1-weighted SE (TR 440 ms, TE 8 ms), multiple enlarged right inguinal nodes (*arrows*); **c** axial FSPGR (TR 255 ms, TE 4.2 ms, flip angle 40°), high signal indicating no USPIO uptake (*arrows*); **d** histologic confirmation of metastatic nodes (cross-section of the vulvar carcinoma. *Inset*: lymph node metastasis; H&E, ×40)

Table 1 Population MRI and histology data (*ca* carcinoma, *LN* lymph nodes)

Patient no.	Final diagnosis	Stage	LN: MRI[a]	LN: Histology[a]	LN staging: MRI
1	Cervical ca.	pT1b1 N0	0/2	0/32	Correct
2	Cervical ca.	pT1b1 N1	0/23	2/14	Micrometastases missed (*n*=2)
3	Cervical ca.	pT1a N0	0/18	0/18	Correct
4	Cervical ca.	pT1b1 N0	1/7	0/41	False-positive hyperplastic node (*n*=1)
5	Cervical ca.	pT1b1 N1	0/10	1/10	5 mm metastasis missed (*n*=1)
6	Undifferentiated sarcoma of cervix	T4	18/37	(No histologic staging)	(Excluded from analysis)
7	Cecal ca.	pT4 N2	6/17	16/20	(Excluded from analysis)
8	Cervical ca.	pT1a Nx	0/6	(No lymphadenectomy)	(Excluded from analysis)
9	Endometrial ca.	pT1b N0	0/9	0/26	Correct
10	Endometrial ca.	pT2b N0	0/2	0/12	Correct
11	Vulvar ca.	pT2 N1	5/18	2/11	Correct
12	Clear-cell ovarian cystadenofibroma, endometrial polyp with hyperplasia	pT1a (borderline)	0/6	(No lymphadenectomy)	(Excluded from analysis)
13	Endometrial ca.	pT1c N0	0/18	1/2 2	Micrometastasis missed (*n*=1)

[a] Malignant/total

crometastases (<5 mm) and one metastasis (5 mm) were missed (Fig. 1). On a nodal basis, the sensitivity score was therefore 0.33 and the specificity score, 0.99.

As for lymph node status on a patient basis, MRI correctly staged four node-negative patients (cervical carcinoma, *n*=2; endometrial carcinoma, *n*=2); it misdiagnosed, as node-negative, two patients with micrometastases (cervical carcinoma. *n*=1; endometrial carcinoma, *n*=1), and one with a malignant lymph node (5 mm cervical carcinoma metastasis); it correctly staged the vulvar carcinoma as node-positive (Fig. 2), and made a false-positive identification in one cervical carcinoma patient. On a patient basis, the sensitivity score was therefore 0.25 and the specificity score, 0.80.

In the patient with a final diagnosis of cecal carcinoma, MRI correctly found multiple lymph node metastas-

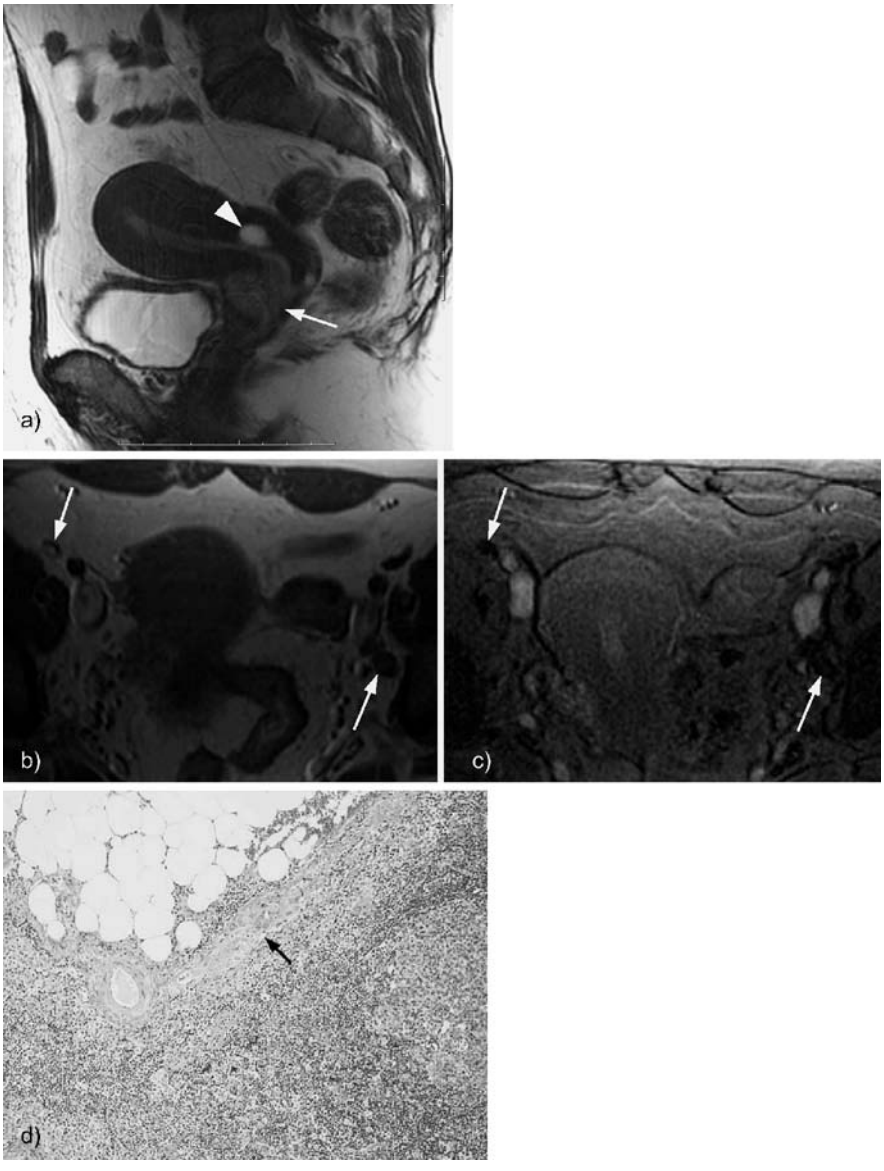

Fig. 3a–d A 38-year-old patient (no. 2, Table 1) with cervical carcinoma (pT1b N1). **a** Sagittal T2-weighted FSE image (TR 6,000 ms, TE 100 ms), primary tumor (*arrowhead*) and nabothian cyst (*arrows*); **b** axial T1-weighted SE (TR 460 ms, TE 8 ms), small lymph nodes (*arrows*) with homogeneous USPIO uptake; **c** axial FSPGR sequences (TR 80 ms, TE 8 ms, flip angle 40°), same; **d** histologic contradiction of MRI findings [micrometastasis (*arrow*) of one lymph node; H&E, ×75]

es (six out of a total of 17 nodes). However, locoregional invasion complicated the task of differentiation from intestinal structures, particularly in the case of metastatic mesenteric nodes, 16 of 20 of which proved malignant on histology (this case had to be excluded from the statistical analysis due to the primary tumor histology, despite the correlation available with the histology).

Discussion

The study shows the feasibility of a same-session imaging strategy for uterine tumors incorporating primary tumor assessment and lymph node mapping. In addition to contrast injection the previous day, lymph node imaging using USPIO-enhanced MRI requires only one additional sequence of about 5 min (axial FSPGR) and is thus feasible in a routine clinical setting. Nodal analysis on the workstation, however, was relatively time-consuming mainly because of the fine-detail mapping (≥2 mm) and the confounding adjacent structures, notably blood vessels.

We saw no serious reactions to USPIO. However, we observed milder and transiently moderate reactions than reported in the literature, despite comparable conditions [22]. The explanation probably lies in coincidental accumulation in our relatively small population.

We confirmed earlier reports that MRI is a reliable technique for T-staging primary uterine tumors. Its only failure was in the case of the cecal carcinoma, due to the

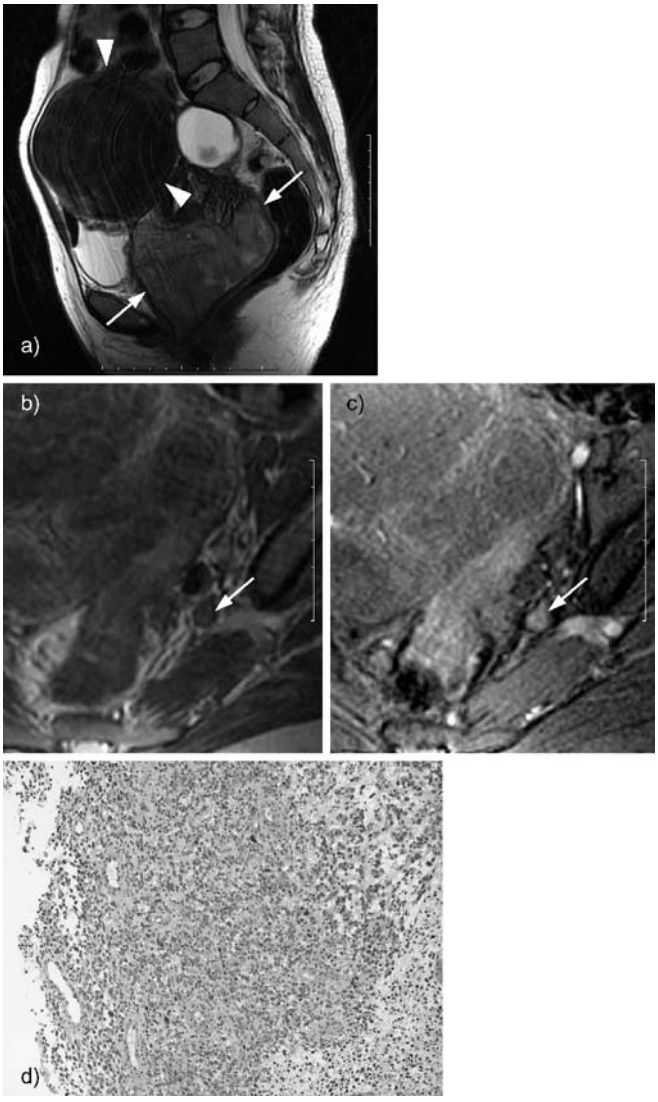

Fig. 4a–d A 36-year-old patient (no. 6, Table 1) with large uterine mass. **a** Sagittal T2-weighted FSE image (TR 4,700, TE 100 ms), leiomyoma (*arrowheads*) and large heterogeneous tumor of the cervix (*arrows*); **b** axial T1-weighted SE (TR 340, TE 8 ms), multiple enlarged iliac lymph nodes with no USPIO uptake, best seen on GRE sequences; **c** axial FSPGR (TR 80 ms, TE 8 ms, flip angle 40°), same; **d** biopsy specimen of the cervical tumor with histologic diagnosis of an undifferentiated sarcoma of the cervix (H&E, ×100)

extensive invasion of adjacent organs. In the suspected uterine sarcoma case, eventually diagnosed as a combination of clear-cell borderline ovarian cystadenofibroma and endometrial hyperplasia, MRI aided the preoperative strategy by identifying an ovarian lesion.

Small nodal metastases are difficult to diagnose on cross-sectional imaging. Metastatic nodes can vary in diameter: not only can the larger nodes not be differentiated from normally reactive nodes of equal size, but signal intensities from metastatic nodes do not differ from those of normal nodes [28]. The specificity of USPIO-enhanced MRI is that it differentiates between enlarged reactive and metastatic nodes [29] and also detects normal-sized metastatic nodes [12]. However, our nodal analysis yielded different sensitivity results than those published in the literature [12, 16, 30]. Although nodal involvement was detected with satisfactory specificity in terms of the literature data, on both a nodal and patient basis, sensitivity was poor. One explanation might lie in our relatively small sample size. Another is that most tumors in our population were at the early stage when lymph node mapping has its greatest impact on therapeutic strategy. Many such patients are likely to be node-negative or have micrometastases. With only one true-positive case (vulvar carcinoma with inguinal metastases) and three false-negative cases at histology, our results must be considered preliminary and interpreted with the appropriate caution. However, in two of the three false-negative cases (cases 2 and 13 in Table 1), the histology showed micrometastases only. Other groups have reported false-negative micrometastatic nodes [30, 31]. Hardware and software constraints prevent MRI from resolving these microstructures for the time being. Contrast dose-dependent susceptibility artifacts in the gradient-echo pulse (GRE) sequences are another reason for missing microlesions [30]. The high sensitivity of GRE imaging to magnetic susceptibility effects can cause overestimation of nodal size [32] and signal homogenization of nodal content [30]. Improved micrometastasis detection rates may therefore have to await the optimization not only of spatial resolution but also of the USPIO-sensitive GRE sequences and contrast dose.

Furthermore, we encountered some problems in nodal analysis that we believe to be pelvis-specific. In contrast to axillary lymph nodes, which are surrounded by fatty tissue and thus readily differentiated from adjacent structures [22], pelvic nodes are typically small and often difficult to distinguish from vessels, the intestinal chemical shift, and USPIO artifacts on GRE sequences. Furthermore, in contrast to the axilla or neck, the region to be imaged (i.e., right and left iliac) is relatively large, resulting in a trade-off between spatial resolution and comprehensiveness when selecting imaging parameters, i.e., field-of-view and slice thickness. Image quality was additionally hampered in some of our cases by gut motion artifacts, a problem which might have been overcome by the use of spasmolytics. Neither operator nor hardware factors are likely to be sufficient explanations for poor sensitivity in that an axillary lymph node study performed under identical conditions achieved markedly superior sensitivity [22].

A further limitation of this preliminary study was our small population of 13 patients, four of whom were excluded from the final statistical analysis. This was simply due to the fact that our referring gynecology depart-

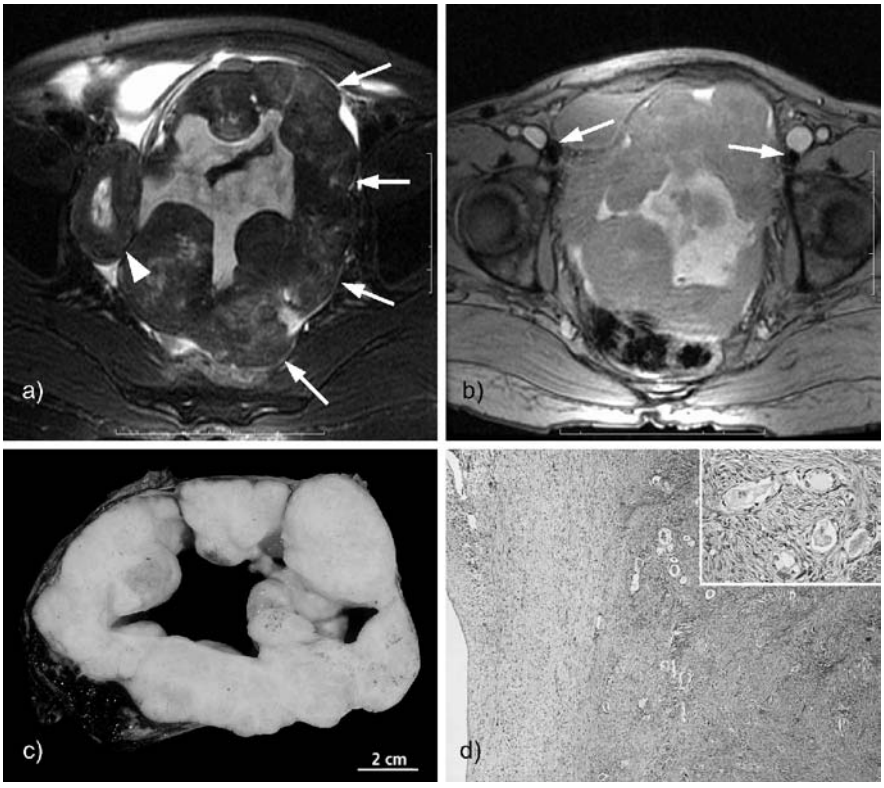

Fig. 5a–d A 56-year-old patient (no. 12, Table 1) with clinically suspected uterine sarcoma. Histology showed an ovarian lesion as well as endometrial hyperplasia. **a** Axial T2-weighted FSE (TR 3,500, TE 100 ms), ovarian lesion (*arrows*) next to uterus (*arrowhead*); **b** axial FSPGR (TR 250, TE 8 ms, flip angle 40°), several normal-size lymph nodes with complete USPIO uptake (*arrows*); **c** resected ovarian tumor 16×10×9 cm: polylobulated mass of 673 g with a centrally located cyst filled with blood (macroscopic specimen); **d** borderline clear-cell cystadenofibroma (H&E, ×30. *Inset*: glandular structures with atypical nuclei and some mitoses without invasion, ×125. Endometrial hyperplasia and polyp not shown)

ment sees 20 times fewer cases of operable uterine tumor than, for example, breast cancer. We had to halt recruitment to our uterine tumor study after exceeding the time limit agreed with the contrast agent company.

In conclusion, USPIO-enhanced MRI of the pelvic nodes is a feasible addition to plain or Gd-enhanced pelvic MRI in patients with uterine tumors. Our preliminary results suggest that it can be a valuable adjunct for preoperative nodal mapping in selected cases. However, further studies in a larger population using improved spatial resolution are needed to evaluate this novel imaging strategy in a clinical setting.

Acknowledgments The study was partly supported by a grant from the Frau Henriette Rossiez-Treichler Legacy, Zurich, Switzerland.

References

1. Grigsby PW, Herzog TJ (2001) Current management of patients with invasive cervical carcinoma. Clin Obstet Gynecol 44:531–537
2. Boronow RC, Morrow CP, Creasman WT et al (1984) Surgical staging in endometrial cancer: clinical-pathologic findings of a prospective study. Obstet Gynecol 63:825–832
3. Lurain JR, Rice BL, Rademaker AW, Poggensee LE, Schink JC, Miller DS (1991) Prognostic factors associated with recurrence in clinical stage I adenocarcinoma of the endometrium. Obstet Gynecol 78:63–69
4. Sevin BU, Nadji M, Lampe B et al (1995) Prognostic factors of early stage cervical cancer treated by radical hysterectomy. Cancer 76:1978–1986
5. Buckley SL, Tritz DM, Van Le L et al (1996) Lymph node metastases and prognosis in patients with stage IA2 cervical cancer. Gynecol Oncol 63:4–9
6. Shepherd JH (1989) Revised FIGO staging for gynaecological cancer. Br J Obstet Gynaecol 96:889–892
7. UICC (2002) TNM Classification of Malignant Tumour. In: Sobin LH, Ch. Wittekind (eds), 6th edn
8. Subak LL, Hricak H, Powell CB, Azizi L, Stern JL (1995) Cervical carcinoma: computed tomography and magnetic resonance imaging for preoperative staging. Obstet Gynecol 86:43–50
9. Kinkel K, Kaji Y, Yu KK et al (1999) Radiologic staging in patients with endometrial cancer: a meta-analysis. Radiology 212:711–718
10. Roy C, Le Bras Y, Mangold L et al (1997) Small pelvic lymph node metastases: evaluation with MR imaging. Clin Radiol 52:437–440
11. Scheidler J, Hricak H, Yu KK, Subak L, Segal MR (1997) Radiological evaluation of lymph node metastases in patients with cervical cancer. A meta-analysis. JAMA 278:1096–1101

12. Bellin MF, Roy C, Kinkel K et al (1998) Lymph node metastases: safety and effectiveness of MR imaging with ultrasmall superparamagnetic iron oxide particles–initial clinical experience. Radiology 207:799–808
13. Kim SH, Kim SC, Choi BI, Han MC (1994) Uterine cervical carcinoma: evaluation of pelvic lymph node metastasis with MR imaging. Radiology 190:807–811
14. Weissleder R, Elizondo G, Wittenberg J, Lee AS, Josephson L, Brady TJ (1990) Ultrasmall superparamagnetic iron oxide: an intravenous contrast agent for assessing lymph nodes with MR imaging. Radiology 175:494–498
15. Rogers JM, Lewis J, Josephson L (1994) Visualization of superior mesenteric lymph nodes by the combined oral and intravenous administration of the ultrasmall superparamagnetic iron oxide, AMI-227. Magn Reson Imaging 12:1161–1165
16. Anzai Y, Blackwell KE, Hirschowitz SL et al (1994) Initial clinical experience with dextran-coated superparamagnetic iron oxide for detection of lymph node metastases in patients with head and neck cancer. Radiology 192:709–715
17. Hamm B (2002) Iron-oxide-enhanced MR lymphography: just a new toy or a breakthrough? Eur Radiol 12:957–958
18. Nguyen BC, Stanford W, Thompson BH et al (1999) Multicenter clinical trial of ultrasmall superparamagnetic iron oxide in the evaluation of mediastinal lymph nodes in patients with primary lung carcinoma. J Magn Reson Imaging 10:468–473
19. Pannu HK, Wang KP, Borman TL, Bluemke DA (2000) MR imaging of mediastinal lymph nodes: evaluation using a superparamagnetic contrast agent. J Magn Reson Imaging 12:899–904
20. Mack MG, Balzer JO, Straub R, Eichler K, Vogl TJ (2002) Superparamagnetic iron oxide-enhanced MR imaging of head and neck lymph nodes. Radiology 222:239–244
21. Stets C, Brandt S, Wallis F, Buchmann J, Gilbert FJ, Heywang-Kobrunner SH (2002) Axillary lymph node metastases: a statistical analysis of various parameters in MRI with USPIO. J Magn Reson Imaging 16:60–68
22. Michel SC, Keller TM, Frohlich JM et al (2002) Preoperative breast cancer staging: MR imaging of the axilla with ultrasmall superparamagnetic iron oxide enhancement. Radiology 225:527–536
23. Harisinghani MG, Saini S, Weissleder R et al (1999) MR lymphangiography using ultrasmall superparamagnetic iron oxide in patients with primary abdominal and pelvic malignancies: radiographic-pathologic correlation. Am J Roentgenol 172:1347–1351
24. Hricak H, Lacey CG, Sandles LG, Chang YC, Winkler ML, Stern JL (1988) Invasive cervical carcinoma: comparison of MR imaging and surgical findings. Radiology 166:623–631
25. Hricak H, Rubinstein LV, Gherman GM, Karstaedt N (1991) MR imaging evaluation of endometrial carcinoma: results of an NCI cooperative study. Radiology 179:829–832
26. Sironi S, Belloni C, Taccagni GL, DelMaschio A (1991) Carcinoma of the cervix: value of MR imaging in detecting parametrial involvement. Am J Roentgenol 156:753–756
27. Sironi S, Colombo E, Villa G et al (1992) Myometrial invasion by endometrial carcinoma: assessment with plain and gadolinium-enhanced MR imaging. Radiology 185:207–212
28. Wang YX, Hussain SM, Krestin GP (2001) Superparamagnetic iron oxide contrast agents: physicochemical characteristics and applications in MR imaging. Eur Radiol 11:2319–2331
29. Vassallo P, Matei C, Heston WD, McLachlan SJ, Koutcher JA, Castellino RA (1995) Characterization of reactive versus tumor-bearing lymph nodes with interstitial magnetic resonance lymphography in an animal model. Invest Radiol 30:706–711
30. Sigal R, Vogl T, Casselman J et al (2002) Lymph node metastases from head and neck squamous cell carcinoma: MR imaging with ultrasmall superparamagnetic iron oxide particles (Sinerem MR) – results of a phase-III multicenter clinical trial. Eur Radiol 12:1104–1113
31. Bellin MF, Beigelman C, Precetti-Morel S (2000) Iron oxide-enhanced MR lymphography: initial experience. Eur J Radiol 34:257–264
32. Tanoura T, Bernas M, Darkazanli A, et al (1992) MR lymphography with iron oxide compound AMI-227: studies in ferrets with filariasis. Am J Roentgenol 159:875–881